

This article was downloaded by:

On: 25 January 2011

Access details: *Access Details: Free Access*

Publisher *Taylor & Francis*

Informa Ltd Registered in England and Wales Registered Number: 1072954 Registered office: Mortimer House, 37-41 Mortimer Street, London W1T 3JH, UK



Separation Science and Technology

Publication details, including instructions for authors and subscription information:

<http://www.informaworld.com/smpp/title~content=t713708471>

Cross-flow microfiltration of dual-sized submicron particles

Kuo-Jen Hwang^a; Keng-Ping Lin^a

^a Department of Chemical Engineering, Tamkang University, Taipei Hsien, Taiwan

Online publication date: 07 June 2002

To cite this Article Hwang, Kuo-Jen and Lin, Keng-Ping(2002) 'Cross-flow microfiltration of dual-sized submicron particles', *Separation Science and Technology*, 37: 10, 2231 – 2249

To link to this Article: DOI: 10.1081/SS-120003511

URL: <http://dx.doi.org/10.1081/SS-120003511>

PLEASE SCROLL DOWN FOR ARTICLE

Full terms and conditions of use: <http://www.informaworld.com/terms-and-conditions-of-access.pdf>

This article may be used for research, teaching and private study purposes. Any substantial or systematic reproduction, re-distribution, re-selling, loan or sub-licensing, systematic supply or distribution in any form to anyone is expressly forbidden.

The publisher does not give any warranty express or implied or make any representation that the contents will be complete or accurate or up to date. The accuracy of any instructions, formulae and drug doses should be independently verified with primary sources. The publisher shall not be liable for any loss, actions, claims, proceedings, demand or costs or damages whatsoever or howsoever caused arising directly or indirectly in connection with or arising out of the use of this material.

CROSS-FLOW MICROFILTRATION OF DUAL-SIZED SUBMICRON PARTICLES

Kuo-Jen Hwang* and Keng-Ping Lin

Department of Chemical Engineering, Tamkang University,
Tamsui, Taipei Hsien 25137, Taiwan

ABSTRACT

The effects of particle size distribution on the cake properties and the performance of cross-flow microfiltration of dual-sized particles are studied. An equation based on the force analysis at the critical condition of particle deposition is derived to relate the filtration rate and the cake properties. The packing porosities of dual-sized particles under various mixing fractions are predicted theoretically in accordance with two limiting conditions, cavern and displacement effects, and are compared to the simulated results and experimental data. The results show that either the theoretical predictions or simulation results agree with the experimental data except in the region near the lowest packing porosity. There has been an overestimation on cake porosity using simulation method and an overestimation using theoretical prediction about 30% near the lowest packing porosity. The average specific filtration resistance of cake can be estimated accurately by substituting the average particle diameter based on the surface area and the Kozeny constant calculated from the cell model into the Kozeny equation. The increase in the mixing fraction of large particles results in a decrease in specific filtration

*Corresponding author. Fax: 886-2-26209887; E-mail: kjhwang@mail.tku.edu.tw

resistance of cake but in an increase in the cake mass. Therefore, the pseudo-steady filtration rate increases with an increase in the mixing fraction of large particles. Once the values of porosity and specific filtration resistance of cakes formed by mono-sized particles are known, the cake properties and the pseudo-steady filtration rates for various mixing ratios of dual-sized particles can be estimated using the proposed theory. The agreements between the calculated results and the experimental data demonstrate the reliability of the proposed method.

Key Words: Cross-flow microfiltration; Submicron particles; Cake properties; Binary particles; Particle deposition; Particle packing

INTRODUCTION

Cross-flow microfiltration has been widely used in many industries for separation of fine particles from liquids. As the cake growth is limited by the shear stress acting on the membrane surface, the filtration rate can be maintained at a higher value for a longer operating time. This mode of filtration has attracted many process engineers and researchers in the field of solid–liquid separation.

Various concentration polarization models have been proposed for predicting the pseudo-steady filtration rates in ultrafiltration (1). These models claimed that a concentration polarization layer might form near the membrane surface during filtration. At a steady state, the particle flux transported by the filtrate towards the membrane surface should be equal to that of back diffusion due to the concentration gradient. However, the parameters used in these models, such as the diffusivity of particles and the particle concentration at the membrane surface, etc., should be obtained by regressing the experimental data.

Since the filtration resistance in microfiltration is mainly determined by the amount and the structure of the filter cake when the particles with a diameter of $0.1\text{--}1.0\text{ }\mu\text{m}$ are to be filtered, to understand how these factors are affected by operating conditions are the essential steps in grasping the problem of filtration. Belfort and co-workers (2,3) have used the hydrodynamic model to analyze the flow field of fluid and the trajectories of particles in a cross-flow filter. Once the concentration profile was solved using the equation of mass-transfer, the transported flux of particles arriving at the membrane surface could be calculated accordingly. Furthermore, the selective deposition of particles in the cross-flow filtration has been discussed (4,5). The external forces exerted on the particle staying on the membrane surface determined whether the particle could deposit

stably or not. Lu and Ju (5) have used a torque balance model to estimate the critical diameter of deposited particles. The particles could deposit stably if their diameters were smaller than the critical value; otherwise, they would roll and be carried away from the membrane surface. By using a force balance model, Lu and Hwang (6) have calculated the critical angle of friction between micron particles staying on the cake surface in a cross-flow filtration system. The probability of particle deposition and the packing structure of particles on the cake surface could be obtained by using the value of critical angle of friction. However, the effects of particle size distribution on the cake structure and the performance of a filtration have not been studied well in these previous research efforts.

In this article, the effects of particle size distribution on the cake properties and the performance of cross-flow microfiltration of dual-sized particles are studied. An equation based on the force analysis is derived to relate the filtration rate, the cake porosity, and the filtration resistance. The packing porosities under various conditions are estimated by theory and simulation method, and are compared to the experimental data. The pseudo-steady filtration rate, the cake porosity, and the specific filtration resistance under various mixing fractions of dual-sized particles can be obtained by the proposed method.

THEORY

Particle Deposition on the Membrane Surface

A two-parallel-plate cross-flow microfiltration system is used in this study. When particles are fed into the filter, some of them are carried by liquid towards the membrane surface during the filtration. When a particle arrives at the membrane or cake surface, whether the particle can deposit stably or be swept away is determined by the forces exerted on it. Figure 1 shows the analyzed system and the forces exerted on a depositing particle. In Fig. 1, particle B is a deposited particle, while particle A is just arriving at the point of contact with particle B. The major forces exerted on particle A include the tangential drag force due to cross-flow of suspension, F_t , the normal drag force due to filtrate flow, F_n , and the net interparticle force, F_i . The inertial lift force and gravity force for such fine particles are negligible compared to the other forces. These forces are analyzed later.

The velocity distribution of a laminar tangential flow in the filter channel can be expressed as (7)

$$u_x = 6u_s \left[\left(\frac{y}{H} \right) - \left(\frac{y}{H} \right)^2 \right] \quad (1)$$

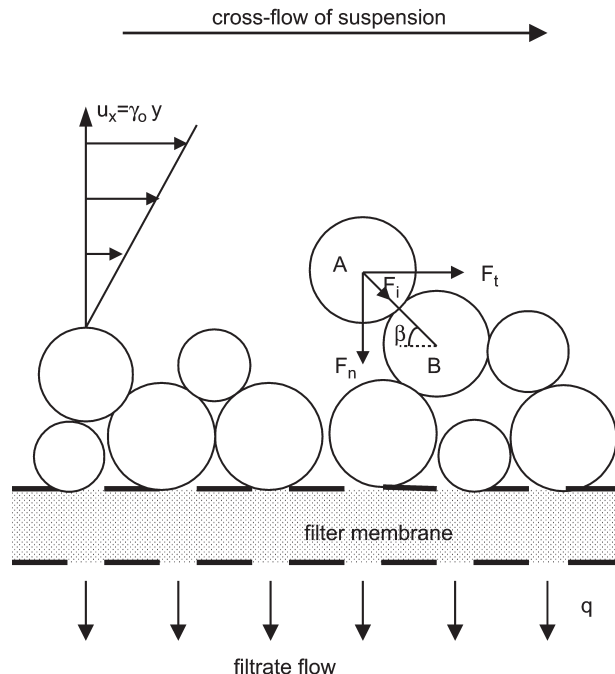


Figure 1. Forces exerted on a depositing particle in the cross-flow microfiltration.

where u_s is the average cross-flow velocity and H the clearance of the filter chamber. Since the velocity of tangential flow near the membrane surface is very slow, and the velocity profile can be reasonably assumed to be linear, the tangential drag force can be estimated by using the modified Stokes law (5), which is given by

$$F_t = \frac{3}{4} \pi \mu d_p^2 \gamma_0 C_1 \quad (2)$$

where d_p is the diameter of particle and γ_0 the shear rate at the membrane surface. The correction factor due to the presence of the membrane or the cake, C_1 , is equal to 1.7009 for a linear shear flow (8). If the roughness of the cake or membrane surface is negligible compared to the clearance of the flow channel, the value of 1.7009 is a suitable approximation. The shear rate at the membrane surface can be estimated using Eq. (1), e.g.,

$$\gamma_0 = \left. \frac{du_x}{dy} \right|_{y=0} = 6u_{s0} \frac{H_0}{(H_0 - L)^2} \quad (3)$$

where the subscript 0 represents the initial value and L the cake thickness. The effects of cake formation on the average cross-flow velocity and the clearance of the filter chamber have been taken into consideration.

The normal drag can also be calculated using the modified Stokes law as the Reynolds number in the filtration direction is very small in most filtrations, that is

$$F_n = 3\pi\mu d_p q C_2 \quad (4)$$

The correction factor, C_2 , can be obtained by (9)

$$C_2 = 0.36 \left(R_t d_p^2 / 4L \right)^{-2/5} \quad (5)$$

As the above equation can be employed for the conditions of thick porous media, the roughness on the cake surfaces is assumed to be neglected compared to the thickness of cakes, and Eq. (5) is a good approximation in most conditions. The total filtration resistance, R_t , can be obtained by summing the filtration resistances of cake and membrane, i.e.,

$$R_t = R_c + R_m = w_c \alpha_{av} + R_m \quad (6)$$

where w_c and α_{av} are the mass and average specific filtration resistance of cake. The value of cake mass can be calculated by the following equation

$$w_c = \rho_s (1 - \varepsilon_{av}) L \quad (7)$$

where ρ_s is the particle density and ε_{av} the average cake porosity.

The interparticle forces can be estimated using the well-known "DLVO theory." On the basis of the pairwise assumption, the major long-range interparticle forces, van der Waals force, and electrostatic force, can be obtained from the results of the authors' previous work (7). As these interparticle forces can be offset by each other due to their opposite acting directions, the value of net interparticle force may be smaller than the drag forces under the conditions of low surface potential or low electrolyte concentration.

Many torque balance and force balance models at the critical condition where particle A can just deposit stably have been proposed by the previous works (5,6). As the net interparticle force is much smaller than the drag forces within the conditions of this study, the balance model can be simplified as

$$F_t = f_c F_n \quad (8)$$

where f_c is a factor which is a function of frictional angle and friction coefficient

between particles. Substituting Eqs. (1)–(7) into Eq. (8) gives

$$f_c = \frac{12.34d_p u_{s0} H_0}{q \left[(\alpha_{av} + R_m/w_c) \rho_s (1 - \varepsilon_{av}) d_p^2 \right]^{2/5} [H_0 - w_c/\rho_s (1 - \varepsilon_{av})]^2} \quad (9)$$

Once the value of f_c is known, Eq. (9) can be used to relate the filtration rate, cake mass, and porosity and specific filtration resistance of cake.

Particle Packing in Cake

Many researchers have focused on the packing porosity of binary particles (10). The theoretical porosity can be derived from the two limiting conditions. One is the cavern effect of small particles. When a few small particles are added into the packing of large particles, small particles will fill into the space among large particles. The packing porosity in such a condition can be estimated by (10)

$$\varepsilon = \frac{\phi_L - 1 + \varepsilon_L}{\phi_L} \quad (10)$$

where ϕ is the volume fraction of particles and the subscript L represents large particles. On the other hand, when a few large particles are added into a large amount of small particles, large particles may displace the packing position of some small particles, and this is the so-called “displacement effect” of large particle. The packing porosity for this condition can be calculated by (10)

$$\varepsilon = 1 - \frac{1 - \varepsilon_S}{1 - \varepsilon_S \phi_L} \quad (11)$$

where the subscript S represents small particles. From Eqs. (10) and (11), one knows that the packing porosity of dual-sized particles is smaller than those of mono-sized, and that the lowest packing porosity for dual-sized particles can be obtained from the cross-point of these theoretical curves, i.e., $\varepsilon = \varepsilon_S \varepsilon_L$.

However, the numerical simulation method has been widely applied to simulate the packing porosity of particles. The authors also proposed a numerical method for simulating the packing structures of particles in filtration (6,11). The drag forces exerted on particles are taken into consideration, and Newton's second law of motion is integrated to estimate the velocity and the position of particle migration during filtration. The details can be referred to from the authors' previous works (6,11).

Basic Filtration Equation

The basic filtration equation can be written as

$$q = \frac{\Delta P}{\mu(w_c \alpha_{av} + R_m)} \quad (12)$$

where ΔP is the filtration pressure. Comparing with the well-known Kozeny equation, the average specific filtration resistance can be expressed as

$$\alpha_{av} = \frac{kS_0^2(1 - \varepsilon_{av})}{\rho_s \varepsilon_{av}^3} \quad (13)$$

where k is the Kozeny constant and S_0 is the specific surface area of particles. For spherical particles under compact packing, the value of k is equal to 5.0. However, k is a function of packing porosity and can be calculated by the free cell model proposed by Happel and Brenner (12), that is

$$k = \frac{2\varepsilon^3}{(1 - \varepsilon) \left\{ \ln \left[\frac{1}{(1 - \varepsilon)} \right] - \left[\frac{1 - (1 - \varepsilon)^2}{1 + (1 - \varepsilon)^2} \right] \right\}} \quad (14)$$

The specific surface area of particles, S_0 , is a function of particle size and cake porosity. The value of S_0 is equal to $6/d_p$ for a single spherical particle. However, for a dual-sized sample, the value of S_0 can be estimated from the average diameter of particles, that is

$$S_0 = \frac{6}{d_{p,av}} = 6 \left(\frac{\phi_L}{d_{p,L}} + \frac{\phi_S}{d_{p,S}} \right) \quad (15)$$

where $d_{p,av}$ is the average diameter based on the surface area of particles.

Once the values of kS_0^2 and cake porosity are obtained, the average specific filtration resistance of cake can be estimated from Eq. (13).

EXPERIMENTAL

Three sizes of polymethyl methacrylate (PMMA) spherical particles with a density of 1210 kg/m^3 were used in cross-flow filtration experiments. Their mean diameters were 0.25, 0.4, and $0.8 \mu\text{m}$, respectively. The dual-sized samples were prepared by mixing particles of 0.25 and $0.8 \mu\text{m}$ with various ratios. Particles were suspended in deionized water to prepare 0.5 wt% suspension. The pH value of the suspension was kept at a value of 7, and the zeta potential of particles under such a condition was -25 mV . The coagulation of particles could be neglected because such value of zeta potential was large enough. The Durapore membrane

manufactured by Millipore Co. with an average pore size of $0.1\text{ }\mu\text{m}$ was used in the filtration. The filtration resistance of the membrane was $2.26 \times 10^{11}\text{ m}^{-1}$ under a filtration pressure of $2 \times 10^4\text{ N/m}^2$.

A schematic diagram of the cross-flow microfiltration system was shown in Fig. 2. The two-parallel-plate filter was constructed with two transparent acrylic plates. The clearance and the length of the filter channel were 1.0×10^{-3} and $5.7 \times 10^{-2}\text{ m}$, respectively. The filtration area used was $1.14 \times 10^{-3}\text{ m}^2$. The temperature of the suspension was kept at 20°C by using a thermostat. In each experiment, the cross-flow velocity was controlled and measured by the rotameter, while the filtration pressure was adjusted to the preset values by the needle valve. The weights of the filtrate were detected by a load cell and recorded on a personal computer during filtration, where values were transformed to filtration rates. The concentrate was recycled back to the suspension tank, and the make-up water with the same amount of filtrate was added into the tank to keep a constant concentration of suspension. As soon as the experiments were terminated, the cake formed on the filter membrane was carefully scrapped and was sent to analyze its wet and dry mass. Once the mass ratio of wet to dry cake was measured, the average porosity and the average specific filtration resistance of the filter cake could be calculated by material balance and the basic filtration equation, respectively. The cake porosity measured by mass analysis was also checked using thermal gravity analysis (TGA). The deviation between these methods was small enough and acceptable. In this study, the cross-flow velocity ranged from 0.1 to 0.6 m/sec, which resulted in a Reynolds number of 100–600.

RESULTS AND DISCUSSION

Figure 3 shows the time courses of filtration rates under various filtration pressures. The used particles are mono-sized, and their average diameter is $0.25\text{ }\mu\text{m}$. In each experiment, the filtration rate attenuates quickly at the beginning of filtration due to the cake formation, and then gradually approaches a pseudo-steady value. This implies that the cake formation is limited by the tangential flow of suspension, and that the operation can be continued for a longer time. It can also be found in Fig. 3 that the increase in filtration pressure increases the filtration rate.

The pseudo-steady filtration rates under various operating conditions are shown in Fig. 4. The solid symbols represent the experimental data for $0.4\text{ }\mu\text{m}$ mono-sized particles. An increase in filtration pressure causes a higher filtration rate due to a higher driving force of filtration, where the trend is similar to the results of Fig. 3. Comparing with these three curves, it can be noticed that the filtration rate increases with an increase in the cross-flow

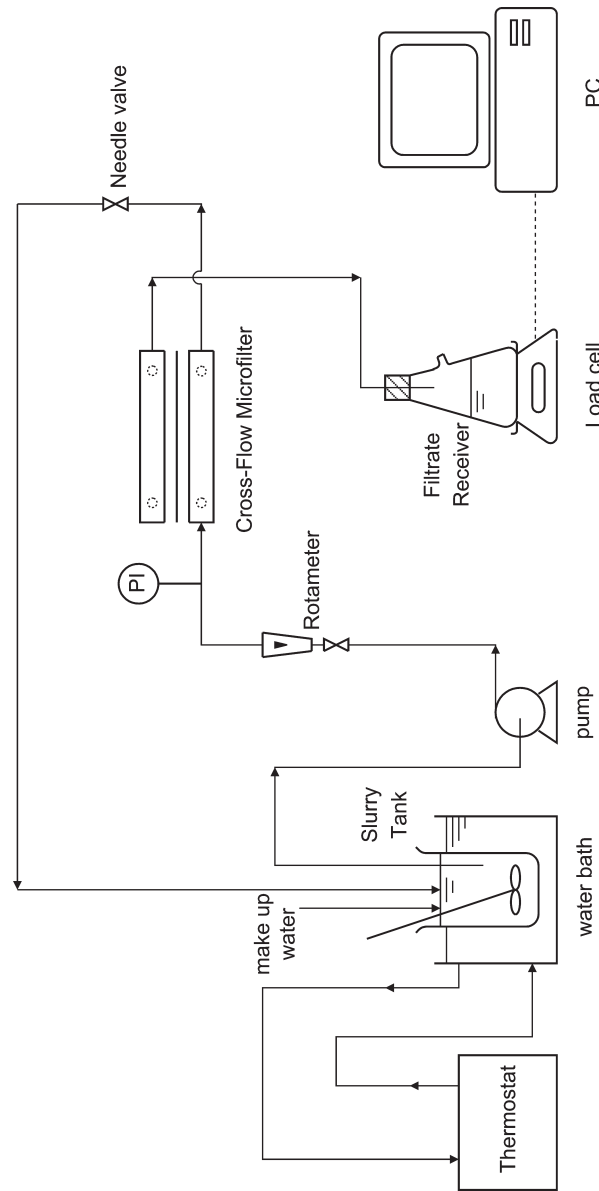


Figure 2. A schematic diagram of the cross-flow microfiltration system.

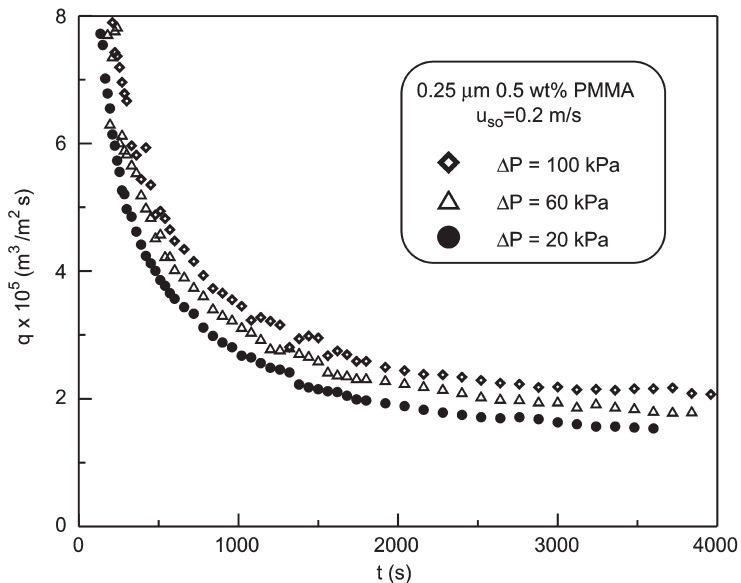


Figure 3. Time courses of filtration rates under various filtration pressures.

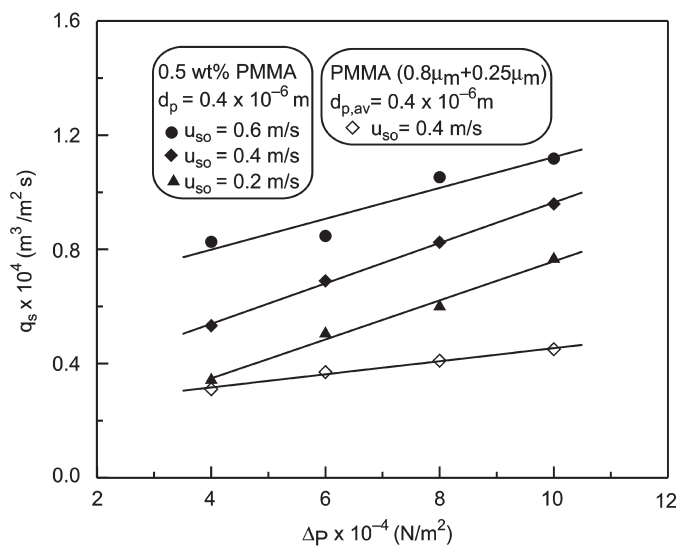


Figure 4. Effects of cross-flow velocity and filtration pressure on the pseudo-steady filtration rate for mono- and dual-sized particles.

velocity. It is because a thinner and loosely packed cake may form under a higher cross-flow velocity due to the higher tangential drag exerted on the depositing particles (6,7). Moreover, two sizes of particles, diameters of 0.8 and 0.25 μm , respectively, are mixed together to prepare a dual-sized particulate sample with a mean diameter of 0.4 μm for experiments. The pseudo-steady filtration rates of this dual-sized sample at $u_{s0} = 0.4 \text{ m/sec}$ under various filtration pressures are shown in Fig. 4 by the symbol of a hollow diamond. The filtration rate of dual-sized particles is smaller than that of mono-sized under the same operating condition, although the average diameter is the same. It can be expected that the cake formed by dual-sized particles has a larger filtration resistance than by mono-sized. In order to understand why this result occurs, the following analyses are carried out.

Prior to predicting the properties of cake formed by dual-sized particles theoretically, the values for mono-sized particles should be known. Figure 5 shows the pseudo-steady filtration rates under various cross-flow velocities for three different sizes of particles. As a higher cross-flow velocity results in a higher tangential drag exerted on particles staying on the membrane surface, the particles will be more easily swept away from the membrane surface. As a result,

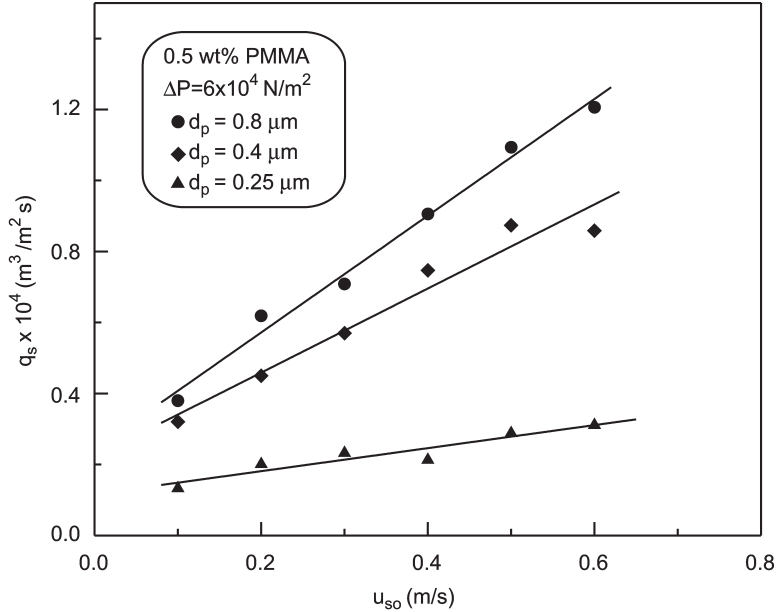


Figure 5. Effect of particle size on the pseudo-steady filtration rate for mono-sized particles.

the filtration rate increases with an increase in the cross-flow velocity. Furthermore, a higher filtration rate will be obtained for larger particles. This result can be expected since the specific filtration resistance of cake is smaller for larger particles [refer to Eq. (9)].

Figure 6 shows the comparison of packing porosities between experimental data and theoretical results under various mixing fractions of large particles. The solid symbols represent the average cake porosity measured under two different filtration pressures. A larger filtration pressure results in lower cake porosity due to the larger solid compressive pressure. It can also be found that the values of packing porosity of dual-sized particles are lower than those of mono-sized, and that the lowest packing porosity occurs at $\phi_L = 0.75$. These phenomena contribute to the cavern effect of small particles and the displacement effect of large particles. The theoretical predictions of these effects for the two operating conditions are also shown in the figures. Each curve is obtained by plotting the calculated results of Eqs. (10) and (11), and these two segments are crossed at the point of the lowest porosity about $\varepsilon_L \varepsilon_S$. The theoretical results agree with the experimental data only when ϕ approaches to 0 or 1. There has been a deviation about 30% at the point of lowest porosity. Therefore, it is demonstrated that the

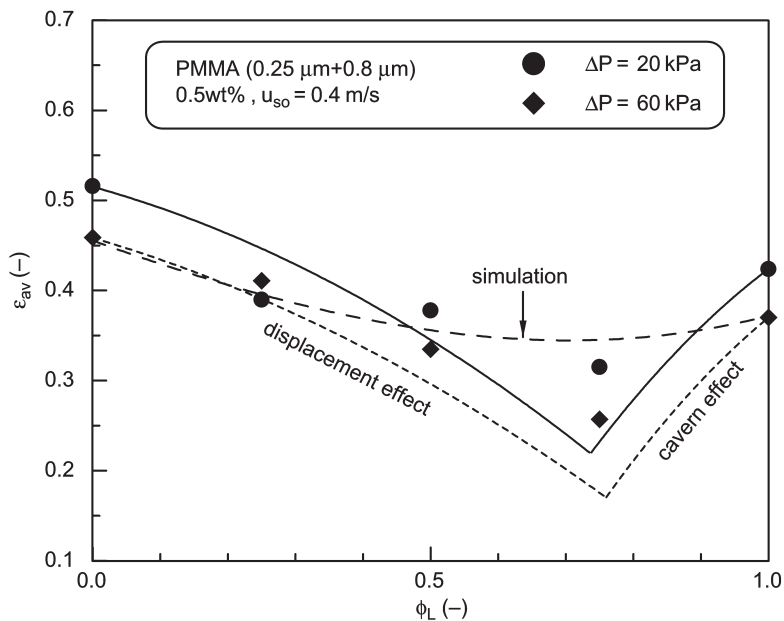


Figure 6. Comparisons of cake porosity among theoretical results, simulated results, and experimental data for various mixing fractions of large particles.

cavern effect can be employed only when a few small particles are added into a large amount of large particles, while the displacement effect can be used for a small value of mixing fraction. Moreover, the simulation results obtained using the numerical method proposed by the authors (6,11) are also shown in Fig. 6 for comparison. The dash curve shown in Fig. 6 is regressed from the simulation results under $u_{s0} = 0.4$ m/sec and $\Delta P = 20$ kPa. The simulated results agree with the experimental data except for the region near the lowest packing porosity. There has been an overestimation of about 30% at the point of the lowest porosity. Due to an inaccuracy, simulation of particle migration is possible in the packing under frictional drag when the mixing fraction is closer to 0.75. However, the simulated results are used for the following calculations of cake properties.

In order to demonstrate the reliability of the proposed theory for particle deposition, experimental data, when the pseudo-steady filtration rates were attained, are substituted into Eq. (9) to calculate the value of f_c . Figure 7 shows the calculated results of f_c under various operating conditions. Although these values are obtained from various cross-flow velocities, filtration rates, filtration pressure, or mixing fractions, the values of f_c remain almost a constant of 8.3.

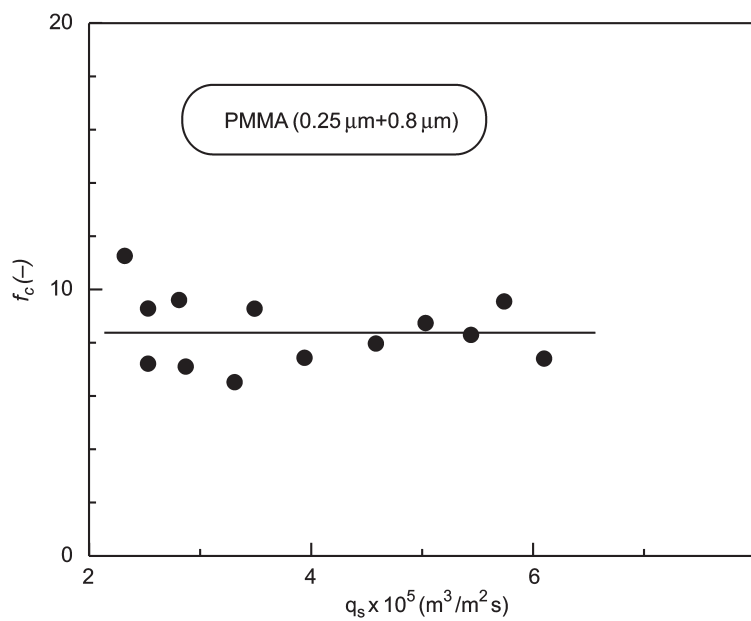


Figure 7. The factor of f_c under various operating conditions.

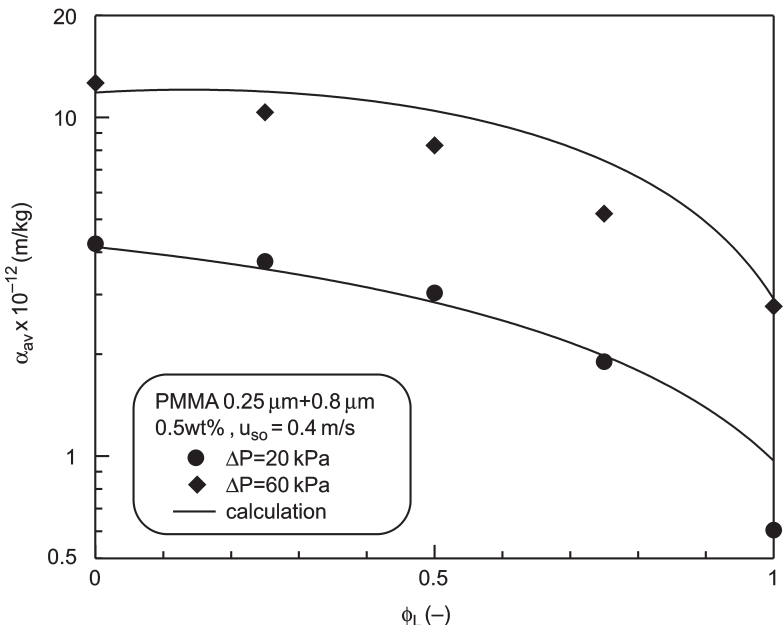


Figure 8. Comparison of average specific filtration resistance of cake between calculated results and experimental data for various mixing fractions of large particles.

Once this value is known, Eq. (9) can be used for predicting the filtration rate or the cake properties in a cross-flow microfiltration.

Figure 8 shows the values of average specific filtration resistance of cake under various mixing fractions for two different filtration pressures. The solid symbols represent the experimental data, while the solid curves are calculated by using Eqs. (13)–(15). From Eq. (13), one knows that the value of α_{av} depends on the porosity of cake and the diameter of particles. A larger filtration pressure results in a higher filtration resistance due to the lower cake porosity. Although the lowest cake porosity exists at $\phi_L = 0.75$, the average specific filtration resistance decreases with increasing the mixing fraction of large particles due to the increase in average particle diameter. The calculated results agree fairly well with the experimental data. This fact implies that the average specific filtration resistance of the cake can be predicted correctly as the cake porosity and the size distributions of particles are known.

Once the values of porosity and specific filtration resistance of cakes formed by two mono-sized particles are known, the factor f_c and the cake

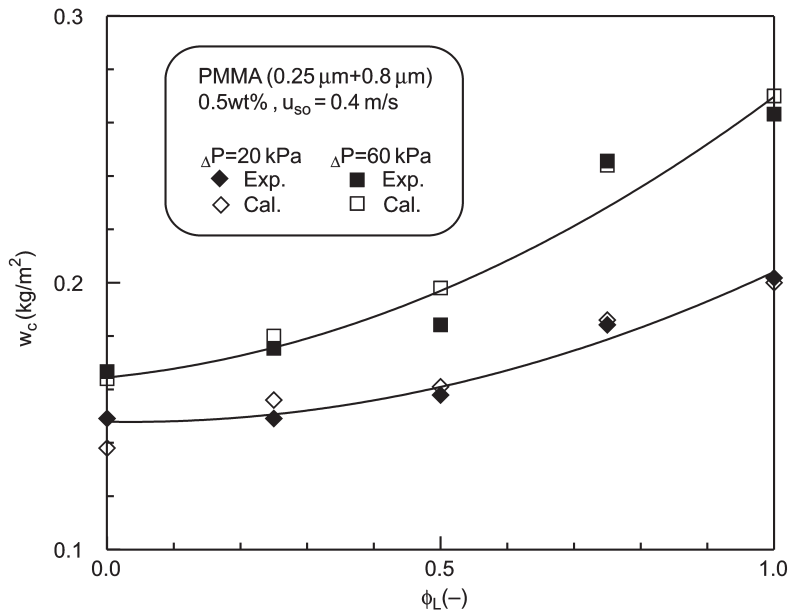


Figure 9. The mass of cake under various mixing fractions of large particles for two different filtration pressures.

properties for various mixing fractions can be estimated using the proposed theory, such as the results of Figs. 6–8. Furthermore, the pseudo-steady filtration rates and cake masses under various conditions can be calculated by solving Eqs. (9) and (12) simultaneously. Figure 9 shows the comparison of cake mass between calculated results and the experimental data under various mixing fractions for two filtration pressures. From the regressed curves of experimental data, it can be observed that an increase in mixing fraction leads to the increase in the cake mass. It is because a large amount of cake may form under a higher filtration rate as the mixing fraction increases. Moreover, the calculated results agree fairly well with the experimental data.

The comparisons of pseudo-steady filtration rate between calculated results and the experimental data are shown in Fig. 10. The solid symbols represent the experimental data, while the hollow symbols represent the results calculated by using Eqs. (9) and (12). The increase in the mixing fraction results in a decrease in the specific filtration resistance of the cake (see Fig. 8), but an increase in the cake mass (see Fig. 9), results in a decrease in the whole filtration resistance of cake. Therefore, it can be observed from Fig. 10 that the filtration rate increases

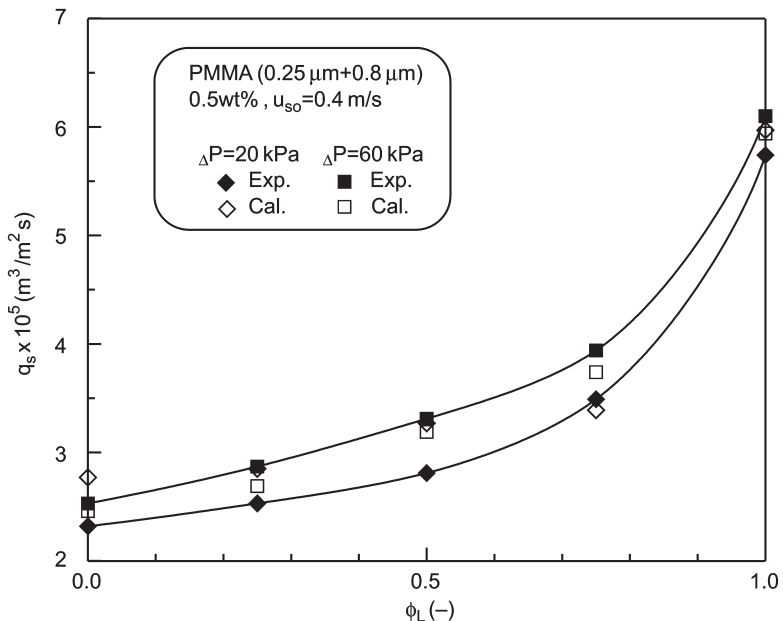


Figure 10. Comparisons of pseudo-steady filtration rates between calculated results and experimental data for various mixing fractions of large particles.

with an increase in the mixing fraction of large particles. The agreements between the calculated results and the experimental data demonstrate the reliability of the proposed method. Once the porosity and the specific filtration of cake are grasped for a given condition, the effects of operating conditions on the cake properties or the filtration rate can be understood by extending the theory proposed by this study.

CONCLUSIONS

The effect of particle size distribution on the performance of cross-flow microfiltration of dual-sized particles has been studied. The theoretical predictions or simulation results of cake porosity agreed fairly well with the experimental data except the region near the lowest packing porosity. A 30% overestimation on cake porosity using simulation method and a 30% underestimation using theoretical prediction occurred near the lowest packing porosity. The average specific filtration resistance of cake was estimated accurately by using the average particle diameter based on surface area and the

Kozeny constant calculated from the cell model. The increase in the mixing fraction of large particles would result in a decrease in the specific filtration resistance of the cake, but an increase in cake mass, results in an increase in the pseudo-steady filtration rate. On the basis of the force analysis at the critical condition of particle deposition, an equation has been derived to relate the filtration rate and the cake properties. Once the values of porosity and specific filtration resistance of cakes formed by mono-sized particles were known, the cake properties and the pseudo-steady filtration rates for various mixing ratios of dual-sized particles could be estimated using the proposed theory. The calculated results agreed fairly well with the experimental data.

NOTATIONS

C_1	correction factor of tangential drag due to the existence of membrane (kg/m ³)
C_2	correction factor of normal drag due to the existence of membrane (kg/m ³)
d_p	diameter of particles (m)
F_n	the normal drag force exerted on particle a due to filtrate flow (N)
F_t	the tangential drag force exerted on particle a due to cross-flow of suspension (N)
f_c	a factor defined in Eq. (8) (-)
H	the clearance of filter channel (m)
k	Kozeny constant (m)
L	cake thickness (m)
ΔP	filtration pressure (N/m ²)
q	filtration rate (m ³ /m ² sec)
q_s	filtration rate at pseudo-steady state (m ³ /m ² sec)
R_c	filtration resistance of cake (m ⁻¹)
R_m	filtration resistance of membrane (m ⁻¹)
R_t	total filtration resistance (m ⁻¹)
S_0	specific surface area of particles (m ² /m ³)
t	filtration time (sec)
u_x	local velocity of fluid in the direction of cross-flow (m/sec)
u_s	average cross-flow velocity of suspension at the inlet of filter (m/sec)
w_c	cake mass (kg/m ²)
y	coordinate whose direction is vertical to the tangential flow of suspension (m)

Greek Letters

α	specific filtration resistance of cake (m/kg)
ε	porosity of cake (-)

ϕ	volume fraction of large particles (-)
γ_0	shear rate at the membrane surface (N/m ²)
μ	viscosity of fluid (kg/m sec)
ρ_s	density of particles (kg/m ³)

Subscripts

av	average value of the property
L	large particles
0	initial condition
S	small particles

ACKNOWLEDGMENTS

The authors express their sincere gratitude to the National Science Council of the Republic of China for its financial support.

REFERENCES

1. Cheryan, M. *Ultrafiltration Handbook*; Technomic Publishing Co.: Pennsylvania, U.S.A., 1986; Chap. 4.
2. Altena, F.W.; Belfort, G. Lateral Migration of Spherical Particles in Porous Flow Channels: Application to Membrane Filtration. *Chem. Eng. Sci.* **1984**, *39* (2), 343–355.
3. Fischer, E.; Raasch, J. Cross-Flow Filtration. *Ger. Chem. Eng.* **1986**, *8*, 211–216.
4. Belfort, G.; Davis, R.H.; Zydny, A.L. The Behavior of Suspensions and Macromolecular Solutions in Crossflow Microfiltration. *J. Membr. Sci.* **1994**, *96*, 1–58.
5. Lu, W.M.; Ju, S.C. Selective Particle Deposition in Cross-Flow Filtration. *Sep. Sci. Technol.* **1989**, *24* (7, 8), 517–540.
6. Lu, W.M.; Hwang, K.J. Cake Formation in 2-D Cross-Flow Filtration. *AIChE J.* **1995**, *41* (6), 1443–1455.
7. Hwang, K.J.; Yu, M.C.; Lu, W.M. Migration and Deposition of Submicron Particles in Crossflow Microfiltration. *Sep. Sci. Technol.* **1997**, *32* (17), 2723–2747.
8. O'Neill, M.E. A Sphere in Contact with a Plane Wall in Slow Linear Shear Flow. *Chem. Eng. Sci.* **1968**, *23*, 1293–1297.
9. Sherwood, J.D. The Force on a Sphere Pulled Away from a Permeable Half-Space. *Physicochem. Hydrodyn.* **1988**, *10*, 3–12.
10. German, R.M. *Particle Packing Characteristics*; Metal Powder Industries Federation: Princeton, NJ, 1989; Chap. 6.

11. Lu, W.M.; Hwang, K.J. Mechanism of Cake Formation in Constant Pressure Filtration. *Sep. Technol.* **1993**, 3, 122–132.
12. Happel, J.; Brenner, H. *Low Reynolds Number Hydrodynamics*; Prentice Hall: Englewood Cliffs, NJ, 1965; Chaps. 6–8.

Received June 2001

Revised December 2001